AWARD NUMBER: W81XWH-19-1-0040

TITLE: PI3K Signaling in Tumor Cells and Stroma Regulates Breast Cancer Metastasis

PRINCIPAL INVESTIGATOR: Jonathan M. Backer, MD

CONTRACTING ORGANIZATION: Albert Einstein College of Medicine

REPORT DATE: JULY 2022

TYPE OF REPORT: FINAL

PREPARED FOR: U.S. Army Medical Research and Development Command
Fort Detrick, Maryland 21702-5012

REPORT DOCUMENTATION PAGE

Form Approved
OMB No. 0704-0188

1. REPORT DATE	2. REPORT TYPE	3. DATES COVERED
JULY 2022	FINAL	3/15/19–3/14/2022

4. TITLE AND SUBTITLE

PI3K Signaling in Tumor Cells and Stroma Regulates Breast Cancer Metastasis

5a. CONTRACT NUMBER

5b. GRANT NUMBER

W81XWH-19-1-0040

5c. PROGRAM ELEMENT NUMBER

6. AUTHOR(S)

Jonathan M. Backer, MD

E-Mail: Jonathan Backer@einsteinmed.org

5d. PROJECT NUMBER

5e. TASK NUMBER

5f. WORK UNIT NUMBER

7. PERFORMING ORGANIZATION NAME(S) AND ADDRESS(ES)

Albert Einstein College of Medicine
1300 Morris Park Avenue
Bronx, NY 10461

8. PERFORMING ORGANIZATION REPORT NUMBER

9. SPONSORING / MONITORING AGENCY NAME(S) AND ADDRESS(ES)

U.S. Army Medical Research and Development Command
Fort Detrick, Maryland 21702-5012

10. SPONSOR/MONITOR'S ACRONYM(S)

11. SPONSOR/MONITOR'S REPORT NUMBER(S)

12. DISTRIBUTION / AVAILABILITY STATEMENT

Approved for Public Release; Distribution Unlimited

13. SUPPLEMENTARY NOTES

14. ABSTRACT

Breast cancer is a major public health problem in the United States, with estimates that 40,000 women die from this disease each year. Tumor metastasis is the major cause of mortality in human breast cancer, and effective treatment of metastatic disease will require a better understanding of the signaling mechanisms that drive breast cancer cell invasion (the ability of tumor cells to move away from the primary tumor and into surrounding tissue). Our data suggests that a specific type of phosphoinositide 3-kinase, called PI3Kbeta, is strongly implicated in breast cancer metastasis. This proposal examines how PI3Kbeta regulates both tumor cells and the stromal cells that modulate tumor cell behavior, leading to increased metastasis. In particular, we have shown that hyperactivation of the PI3K pathway may supplant the role of PI3Kbeta in tumor cells. In addition, we have identified novel roles for PI3Kbeta in macrophages and platelets during the induction of tumor cell matrix degradation and invasion. Our study could establish PI3Kbeta as an important new drug target for the treatment of metastatic disease.

15. SUBJECT TERMS

NONE LISTED

16. SECURITY CLASSIFICATION OF:			17. LIMITATION OF ABSTRACT	18. NUMBER OF PAGES	19a. NAME OF RESPONSIBLE PERSON
a. REPORT	b. ABSTRACT	c. THIS PAGE			USAMRDC
Unclassified	Unclassified	Unclassified	Unclassified	20	19b. TELEPHONE NUMBER *(include area code)*

TABLE OF CONTENTS

1. INTRODUCTION: The overall focus of this research is to define the mechanisms that drive breast cancer metastasis. The work is based on our preliminary data showing that a single isoform of phosphoinositide 3-kinase, PI3Kβ, is required for two distinct cellular structures: macropinosomes and invadopodia. We proposed the hypothesis that macropinocytosis is required for invadopodia formation, by the targeting of integrins from the dorsal surface of the cell to ventral invadopodia. We further proposed, based on data using primary macrophages from mutant PI3Kβ mice, that loss of PI3Kβ signaling in stromal cells will inhibit metastasis *in vivo.* Thus, these studies will provide new mechanistic insights into tumor cell invasion, and new physiological insights into PI3Kβ signaling in an animal model of breast cancer metastasis.

2. KEYWORDS: Metastasis, phosphoinositide 3-kinase, macropinocytosis, invasion, invadopodia, integrins, mouse models.

3. ACCOMPLISHMENTS:

What were the major goals of the project?

a. Define the coupling between macropinosomes and podosomes.

i. Examine invadopodia formation/function under conditions of macropinosome inhibition. Target date: March 2020. Completed date: October 2020. Hypothesis invalidated.

ii. Analyze the regulation of integrin signaling/trafficking by PI3Kβ. Target date: September 2020. Completed date: December 2020. Hypothesis invalidated.

iii. Regulation of the invadopodia proteome by macropinocytosis

Target date: February 2022. % completed: 100%. Hypothesis invalidated.

b. Test the role of stromal PI3Kβ in tumor growth and metastasis.

i. Tumor growth in WT and mutant PI3Kβ mice

Target date: March 2021. % completed: 20%.

ii. Tumor invasion/metastasis in WT and mutant PI3Kβ mice

Target date: March 2022. % completed: 50%.

iii. Role of PI3Kβ in extravasation

Target date: March 2020. % completed: 50%.

iv. PI3Kβ macrophage-specific mutant mice.

Target date: March 2022. % completed: 0%.

What was accomplished under these goals?

a. Define the coupling between macropinosomes and podosomes.

i. Examine invadopodia formation/function under conditions of macropinosome inhibition. We have tested two of target proteins, Rabankyrin-5 and Vps34. For both proteins, we needed to establish knockdown or inhibition, and then measure the effects on macropinocytosis and gelatin degradation.

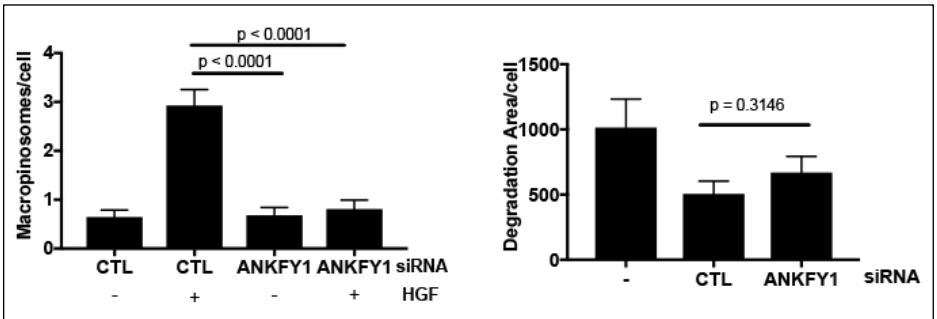

Figure 1. Left: Macropinocytosis is inhibited by Rabankyrin-5 knockdown. Right: Gelatin degradation is unaffected by Rabankyrin-5 knockdown.

Rabankyrin 5. We used pooled siRNA oligos (Dharmicon) to knock down Rabankyrin-5. Quantitation of western blots showed a 70% knockdown after 72h (data not shown). Rabankyrin-5 knockdown caused a nearly complete block of HGF-stimulated macropinocytosis in MDA-MB-231 cells, but had no effect on gelatin degradation (Figure 1). Similarly, inhibition of the Class III PI 3-kinase Vps34, abolished HGF-stimulated macropinocytosis but had no effect on gelatin degradation (Figure 2). We also tested a third drug, imipramine, a tricyclic antidepressant that has been reported to block

macropinocytosis, (Lin et al, Br. J. Pharmacol.175:3640, 2018), but did not detect any inhibition of macropinocytosis (data not shown).

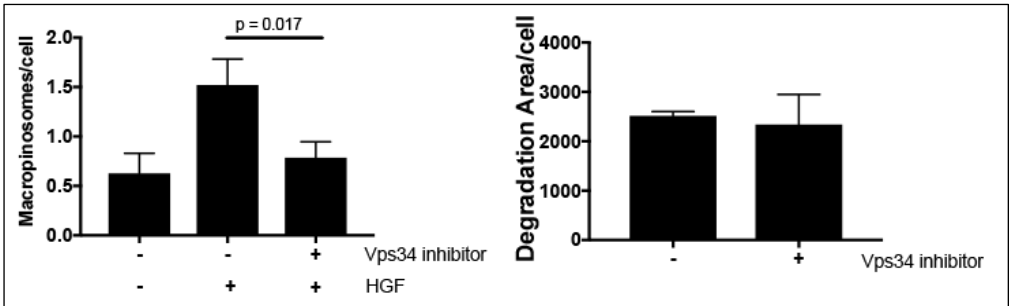

Figure 2. Left. Macropinocytosis is attenuated by inhibition of Vps34. Right. Gelatin degradation in unaffected by inhibition of Vps34.

Our hypothesis in these experiments was that if macropinocytosis served as a critical transporter of regulatory proteins to invadopodia, then inhibitors of macropinocytosis would also inhibit gelatin degradation. Our data argues strongly against this hypothesis, as two macropinocytosis inhibitors had no effect on invadopodial function.

ii. Visualize macropinocytosis-dependent trafficking of proteins to invadopodia.

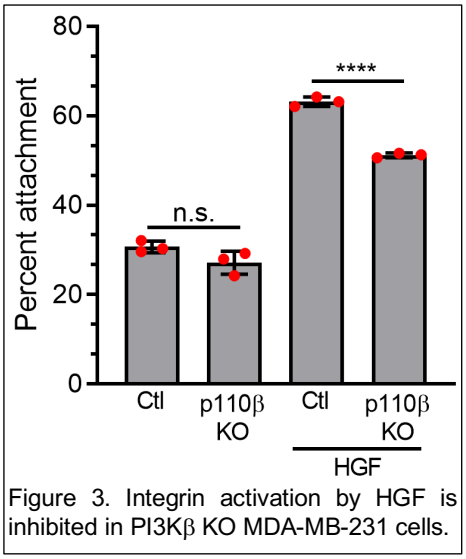

Figure 3. Integrin activation by HGF is inhibited in PI3Kβ KO MDA-MB-231 cells.

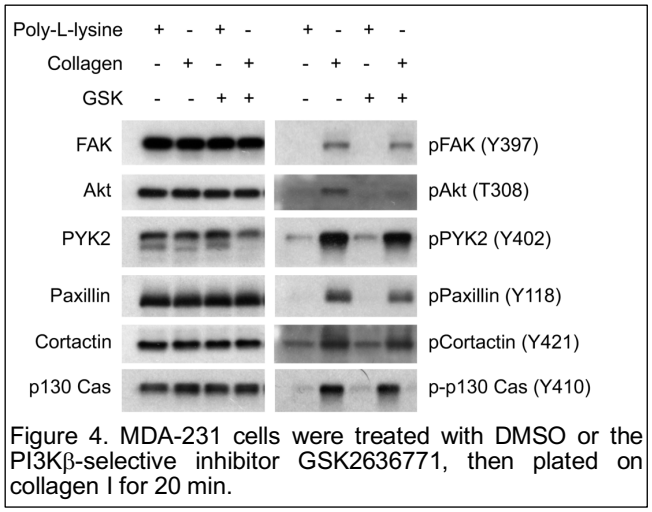

Figure 4. MDA-231 cells were treated with DMSO or the PI3Kβ-selective inhibitor GSK2636771, then plated on collagen I for 20 min.

Our published data show that PI3Kβ is required for integrin-dependent cellular responses in tumor cells, and we have also shown that PI3Kβ is required for HGF-stimulated macropinocytosis in MDA-MB-231 cells We have found that HGF stimulates inside-out integrin activation in MDA-MB-231 cells, as measured by an increase in adhesion to fibronectin (Fig. 3). While this response is reduced in PI3Kβ KO MDA-MB-231 cells, the reduction is fairly small. We also measured signaling responses to integrin activation by measuring the phosphorylation of known integrin effectors (1-6) after plating MDA-MB-231 cells on collagen I. As shown in Fig. 4, integrin-stimulated kinase signaling to FAK, Pyk2, paxillin, cortactin and p130Cas were unaffected by inhibition of PI3Kβ with the selective inhibitor GSK2636771; Akt phosphorylation was partially inhibited as expected (7). These data are not consistent with a major role for PI3Kβ-mediated macropinocytosis in integrin signaling in breast cancer cells.

iii. Regulation of the invadopodia proteome by macropinocytosis.

These experiments were designed to test the mechanism by which macropinocytosis regulates invavopodia. Given that our data did not support the original hypothesis, we did not pursue this proteomic experiment, and instead focused on the role of PI3Kβ in tumor cell- stromal interactions.

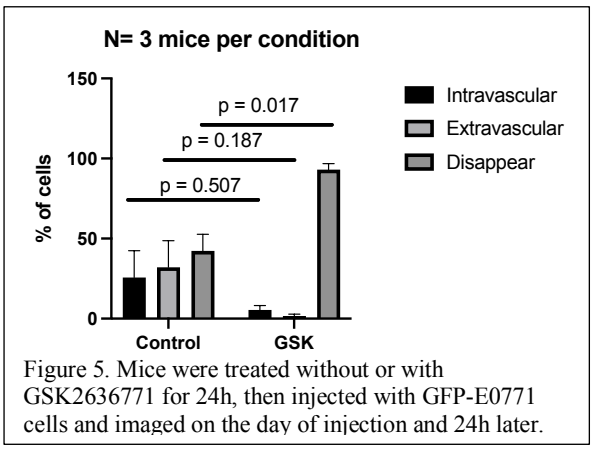

Figure 5. Mice were treated without or with GSK2636771 for 24h, then injected with GFP-E0771 cells and imaged on the day of injection and 24h later.

b. Test the role of stromal PI3Kβ in tumor growth and metastasis.

As discussed in the 2021 progress report, we had proposed to study the role of stromal PI3Kβ during metastasis in vivo, using our C57Bl/6 mice and the syngeneic E0771 tumor line. Orthotopic injection of E0771 cells into the mammary fat pad of C57Bl/6 mice, tumor take is seldom better than 50%, and tumor growth is extremely variable. Even with large tumors, we find that spontaneous metastasis to the lung is low. After a major effort to improve the system by variations in injection

site, tumor cell number, and presence of Matrigel, we decided to switch to tail vein injections to model tumor cell extravasation. In collaboration with David Entenberg (Dept. Pathology), we made use of a novel implantable imaging window, which makes it possible to follow the fate of GFP-labeled tumor cells in the lung using multiphoton microscopy; fiducial marks on the lung window make it possible to observe the same fields of view over multiple days. In preliminary experiments, mice were implanted with the lung imaging window, treated mice for 24h with the PI3Kβ-selective inhibitor GSK2636771 or vehicle, and then injected GFP-E0771 cells. Cells were imaged on the day of injection and after 24h. In control mice, 25% of cells remain in the vasculature after 24h, and 25% extravasate into the lung parenchyma. However, in inhibitor-treated cells, virtually all of the injected cells disappeared after 24h, due to cell death or loss to the circulation.

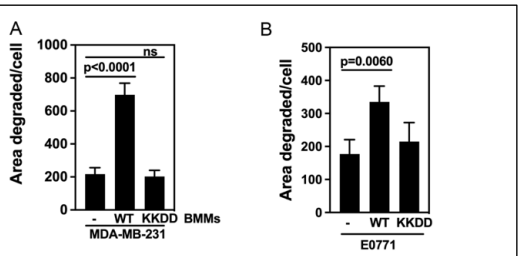

Figure 6: Gβγ binding to PI3Kβ is required for BMM-induced tumor cell gelatin degradation. A) Gelatin degradation was measured in MDA-MB-231 cells co-cultured with or without WT or mutant BMMs. B) Gelatin degradation was measured in E0771 cells co-cultured with or without WT or mutant BMMs.

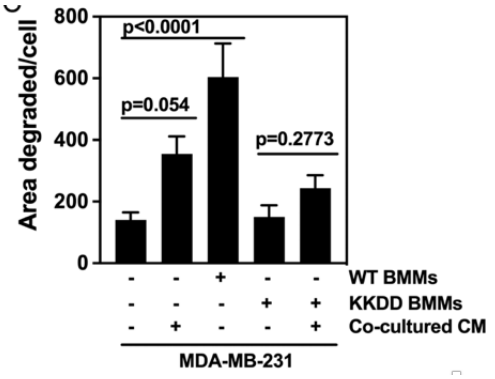

Figure 7: BMM conditioned media fails to rescue the induction of tumor cell gelatin degradation by KKDD BMMs. Gelatin degradation was measured in MDA-MB-231 cells co-cultured with or without WT or KKDD BMMS in the presence or absence of CM derived from BMM-tumor cell co-cultures. Data are the mean ± SEM from 3 independent experiments.

While these data strongly suggest that PI3Kβ plays a critical role in metastasis, we cannot differentiate between the effects of GSK263671 on stromal cells versus the tumor cells themselves. We therefore tried to repeat these experiments in our mutant PI3Kβ knock-in mice. Unfortunately, 3 of 3 mice failed to survive the lung implantation surgery (as compared to 100% survival in control mice). While the reason for the poor survival in mutant PI3Kβ mice is not yet known, we have been so far unable to continue these experiments. Given our problems with the in vivo experiments, we pursued in vitro studies on the role of PI3β in tumor cell invasion.

i. Tumor cell matrix degradation. We have previously shown that formation of mature degradation-competent invadopodia in breast cancer cells requires the PI3Kβ isotype. To explore this requirement in more detail, we tested whether the selectivity for PI3Kβ is preserved under conditions of mutational increases in PI3K activity. In breast cancer cells where PI3Kβ is inhibited, short chain diC8-PIP_3 rescues gelatin degradation in a SHIP2-dependent manner, whereas rescue by diC8-$PI(3,4)P_2$ was independent of SHIP2. Surprisingly, expression of either activated PI3Kα or PI3Kβ mutants rescued the effects of PI3Kβ inhibition. In both cases, gelatin degradation was SHIP2-dependent. These data confirm the requirement for PIP_3 conversion to $PI(3,4)P_2$ for invadopodia function, and suggest that the selectivity for distinct PI3K isotypes during tumor cell invasion maybe obviated by mutational activation of the PI3K pathway. These data were published in FEBS Letters in 2022 (see attached pdf).

Figure 8: IL8 does not rescue BMM-induced tumor cell gelatin degradation. A) IL8 secretion by MDA-MB-231 cells was measured following co-culture with WT or KKDD BMMs by ELISA. Data was normalized to IL8 secretion during co-culture with WT BMMS. B) Gelatin degradation was measured in MDA-MB-231 cells co-cultured with or without WT or KKDD BMMS in the presence or absence of recombinant IL8. Data are the mean ± SEM from 3 independent experiments.

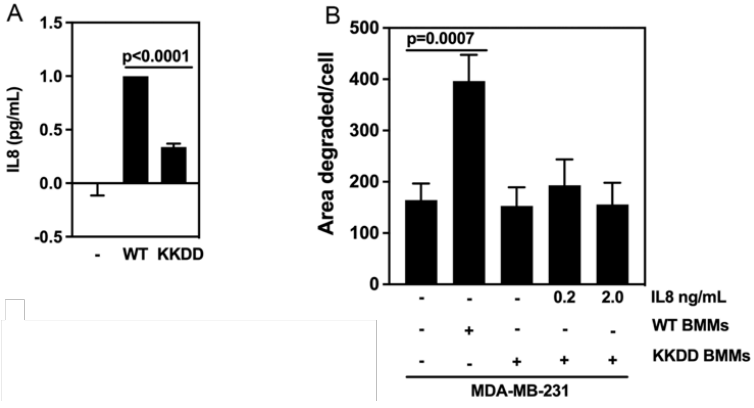

ii. PI3Kb signaling in tumor cell-macrophage interactions. In direct support of our hypothesis that stromal-cell PI3Kb support tumor cell invasion, we showed that WT but not PI3Kb mutant macrophages enhance matrix

degradation by tumor cells; this experiment is performed using crosslinked-gelatin matrix, which the macrophages are unable to degrade. We measured matrix degradation by both human (MDA-MB-231) and mouse (E0771) cells incubated for 17h with primary bone marrow-derived macrophages from WT or PI3Kβ mutant mice ; in both cases, mutation of macrophage PI3Kβ abolished the stimulation (Fig. 6). To explore the mechanisms by which macrophages induce gelatin degradation by tumor cells, we tested the effects of conditioned medium (CM) collected from WT BMMs on gelatin degradation by MDA-MB-231 cells. CM from WT BMMs, either alone or in the presence of KKDD BMMs, did not stimulate gelatin degradation by MDA-MB-231 cells (data not shown). Similarly, conditioned medium from BMM-MDA-MB-231 cell co-cultures failed to rescue tumor cell gelatin degradation in the presence of KKDD BMMs (Fig. 7). Interestingly, co-culture CM did increase gelatin degradation by MDA-MB-231 cells in the absence of BMMs.

We tested several other potential mechanisms for macrophage stimulation of matrix degradation. We had previously used antibody arrays to show that WT, but not PI3Kβ mutant macrophages, stimulated IL8 secretion by tumor cells; we confirmed this result by ELISA (Fig 8A). However, addition of exogenous IL8 did not rescue the induction of tumor cell matrix degradation by mutant BMMs (Fig. 8B). We also measured induction of NF-kB signaling, which has been implicated in macrophage-tumor cell paracrine signaling. While incubation of MDA-MB-231 cells with BMMs did stimulated NF-kB, we observed no differences when using WT versus mutant PI3Kβ BMMs (data not shown). Thus, differences in NF-kB signaling do not explain the reduced response to mutant BMMs.

Fig. 9. MDA-MB-231 cells were incubated with WT or mutant platelets for 40h, and tumor cell invasion was measured.

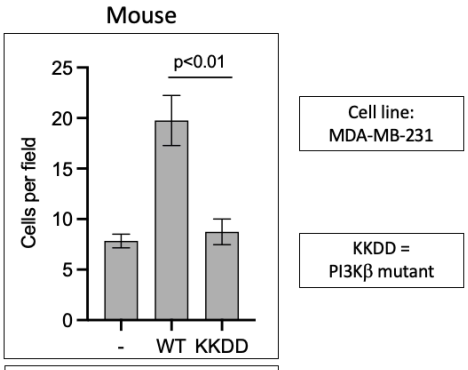

To test additional mechanisms for the loss of response to PI3Kβ mutants macrophages, we have performed RNAseq analysis of co-cultures of MDA-MB-231 cells with WT or mutant BMMs. We observe clear differences in the transcriptional responses of WT or mutant BMMs to tumor cells; analysis of these data is currently underway.

ii. PI3Kβ signaling in tumor cell-platelet interactions.

Platelet binding to circulating tumor cells is necessary for metastatic dissemination. Previous studies have shown that incubation of platelets with tumor cells for 40h enhances the invasion of the tumor cells in Matrigel invasion assays. To optimize this assay for MCF10A breast epithelial cells, we incubated the tumor cells with freshly isolated human platelets at varying rations for 40h, washed to remove the platelets, and then measured tumor cell invasion toward serum in an Matrigel invasion assay. Invasion was increased by platelets in a dose-dependent manner, with a 6-fold increase in invasion with platelets in 50-fold excess over MCF10A cells (data not shown). We then extended our analysis to MDA-MB-231 tumor cells. Platelets induced a 2-fold increase in invasion, which was abolished in platelets from PI3Kβ mutant mice (Fig. 9).

Fig. 10. FACS analysis of platelet activation by P-selectin expression.

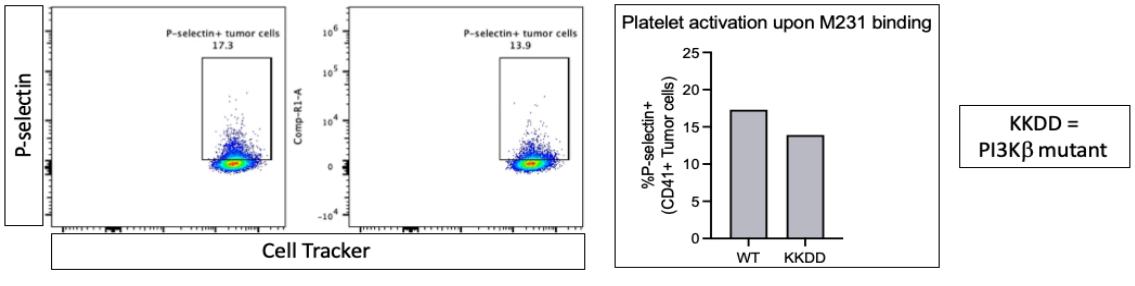

PI3Kβ is required for activation of platelets by collagen and ADP (data not shown). We therefore measure the ability of PI3Kβ mutant platelets to bind and be activated by tumor cells. Surprisingly, we found no difference in the binding of PI3Kβ mutants platelets to MDA-MB-231 and other breast cancer lines (data not shown). We also failed to detect any differences in the activation of platelets from WT or mutant mice in response to tumor cell binding (Fig. 10). These data suggest that loss of

PI3Kβ in platelets may lead to changes in their repertoire of secreted proteins or membrane bound proteins that could interact with tumor cells. Proteomic analysis of thrombin-stimulated cell surface proteins in WT or mutant PI3Kβ failed to detect significant differences; we are now analyzing the repertoire of secreted proteins in WT and mutant PI3Kβ platelets.

Table 1. PI3Kβ-dependent secretion of tumor cell proteins in response to platelets.

Name	Function	Fold	P value
Amphiregulin	EGFR ligand; breast cancer	5.1	0.003
ADAM9	Protease – sheddase for EGF ligands	4.3	3.7E-08
ANGPTL-4	Vascular permeability; breast cancer	3.9	6.1E-08
TSP-4	Gastric and hepatic carcinoma	3.7	0.002
VEGF-C	Breast cancer metastasis	3.4	7.2E-07
IL8	Immune cell recruitment; breast cancer metastasis	3.1	2.4E-07
HDGF	Breast cancer metastasis	3.1	2.4E-07

In another approach to defining the mechanism by which platelet PI3Kβ regulates tumor cell response, we performed a proteomic analysis of the secretome of co-cultures between MCF10A cells and WT or PI3Kβ murine mutant platelets. While we hoped to be able to distinguish proteins secreted from murine platelet and human tumor cells, in fact it was difficult to unambiguously identify secreted mouse proteins. We were, however, able to identify a number of human proteins whose secretion from MCF10A cells is regulated by platelet PI3Kβ (Table 1). These include multiple proteins implicated in tumor metastasis. Studies on ongoing to test the role of these proteins in platelet-induced invasive behavior in tumor cells.

What opportunities for training and professional development has the project provided?

A student in the lab, Ryan Graff, was successful in obtaining an F30 fellowship based on the PI3Kβ-platelet work (NCI 1 F30 CA265236).

How were the results disseminated to communities of interest?

The work on PI3K isotype selectivity during tumor cells invasion was published in FEBS Letters (PMID 3499002). The paper was featured as an "Editor's Choice" in the Feb 2022 issue.

The work on PI3Kβ signaling in macrophages and platelets, and their effect on tumor cell behavior, is in preparation.

What do you plan to do during the next reporting period to accomplish the goals?

Nothing to Report.

4. IMPACT:

What was the impact on the development of the principal discipline(s) of the project?

Our studies show that PI3Kβ plays a critical role in both platelets and macrophages with regard to their interactions with breast cancer cells. These in vitro studies, along with our in vivo studies showing that the PI3Kβ inhibitor GSK263671 inhibits tumor cells extravasation, serve as preclinical evidence for the utility of PI3Kβ inhibition in the treatment or prevention of breast cancer metastasis. However, our published work also suggests that hyperactivation of PI3K signaling can supplant the requirement for PI3Kβ in tumor cell invasion, suggesting that the use of PI3Kβ-selective inhibitors may be limited in tumors expressing activated mutations in PI3Kα.

What was the impact on other disciplines?

Nothing to report.

What was the impact on technology transfer?

Nothing to report.

What was the impact on society beyond science and technology?

Nothing to report.

5. CHANGES/PROBLEMS:

Nothing to report.

Changes in approach and reasons for change

Nothing to report.

Actual or anticipated problems or delays and actions or plans to resolve them

Nothing to report.

Changes that had a significant impact on expenditures

Nothing to report.

Significant changes in use or care of human subjects, vertebrate animals, biohazards, and/or select agents

Nothing to report.

Significant changes in use or care of human subjects

Nothing to report.

Significant changes in use or care of vertebrate animals.

Nothing to report.

6. Products

Publications:

Charles T. Jakubik, Claire C. Weckerly, Gerald R.V. Hammond, Anne R. Bresnick, Jonathan M. Backer. PIP_3 abundance overcomes PI3K signaling selectivity in invadopodia. FEBS Letters 2022 596:417-426

7. PARTICIPANTS AND OTHER COLLABORATING ORGANIZATIONS.

Name:	Jonathan Backer, MD
Project Role:	PI
ID	Orchid ID 0000-0002-0360-5692
Nearest person month worked	6
Contribution:	Directed project
Funding support	See Other Support, below
Name:	Anne Bresnick, PhD
Project Role:	Co-Investigator
ID	Orchid ID 0000-0003-1674-4568
Nearest person month worked	6
Contribution:	Co-directed project
Funding support	See Other Support, below
Name:	Charles Jakubik
Project Role:	Graduate student
ID	
Nearest person month worked	12
Contribution:	Performed macrophage experiments
Funding support	NIH T32 GM7288

Name:	Ryan Graff
Project Role:	Graduate student
ID	Orchid ID 0000-0003-4227-546X
Nearest person month worked	12
Contribution:	Performed platelet experiments
Funding support	1 F30 CA265236

Change in other support:

Title: S100A4 and Metastasis: The S100A4 Receptor
Project Number: 35220H
Name of PD/PI: Bresnick, A.R., Backer J.M.
*Source of Support: Montefiore Einstein Cancer Center Price Family Foundation Pilot Project Awards
Project/Proposal Start and End Date: (MM/YYYY) (if available): 11/2021-11/2023
* Total Award Amount (including Indirect Costs): $200,000

Title: Platelet PI3Kbeta regulation of metastasis
Project Number: 1 F30 CA265236
Name of PI" Graff, Ryan
Source of Support: NCI
Project dates: 12/22/21-12/20-24
Total award amount: $51,036

Other Organizations:
Name: Department of Cell Biology, University of Pittsburgh School of Medicine (J. Hammond, PhD)
Location: Pittsburgh, PA
Contribution: Collaboration.

8. Special Reporting Requirements
Not applicable

9. Appendices: attached manuscript.

FEBS Letters

FEBS PRESS science publishing by scientists

EDITOR'S CHOICE

PIP_3 abundance overcomes PI3K signaling selectivity in invadopodia

Charles T. Jakubik[1], Claire C. Weckerly[2], Gerald R.V. Hammond[2], Anne R. Bresnick[1] and Jonathan M. Backer[1,3]

1 Department of Biochemistry, Albert Einstein College of Medicine, Bronx, NY, USA
2 Department of Cell Biology, University of Pittsburgh School of Medicine, PA, USA
3 Department of Molecular Pharmacology, Albert Einstein College of Medicine, Bronx, NY, USA

Correspondence
A. R. Bresnick and J. M. Backer, Departments of Biochemistry and Molecular Pharmacology, Albert Einstein College of Medicine, 1300 Morris Park Avenue, Bronx, NY, USA
Tel: 718-430-2741; 718-430-2153
E-mails: anne.bresnick@einsteinmed.edu; jonathan.backer@einsteinmed.edu

(Received 19 October 2021, revised 7 December 2021, accepted 16 December 2021, available online 12 January 2022)

doi:10.1002/1873-3468.14273

Edited by Lukas Alfons Huber

PI3Kβ is required for invadopodia-mediated matrix degradation by breast cancer cells. Invadopodia maturation requires GPCR activation of PI3Kβ and its coupling to SHIP2 to produce $PI(3,4)P_2$. We now test whether selectivity for PI3Kβ is preserved under conditions of mutational increases in PI3K activity. In breast cancer cells where PI3Kβ is inhibited, short-chain diC8-PIP_3 rescues gelatin degradation in a SHIP2-dependent manner; rescue by diC8-$PI(3,4)P_2$ is SHIP2-independent. Surprisingly, the expression of either activated PI3Kβ or PI3Kα mutants rescued the effects of PI3Kβ inhibition. In both cases, gelatin degradation was SHIP2-dependent. These data confirm the requirement for PIP_3 conversion to $PI(3,4)P_2$ for invadopodia function and suggest that selectivity for distinct PI3K isotypes may be obviated by mutational activation of the PI3K pathway.

Keywords: invadopodia; matrix degradation; PI 3-kinase

Invadopodia are protrusive structures that degrade extracellular matrix (ECM) and promote tumour cell invasion into surrounding tissue. Invadopodia are required for numerous steps in the metastatic cascade, including local invasion, intravasation and extravasation [1,2]. Invadopodia formation occurs in a step-wise manner [3]. Invadopodia precursors, which cannot degrade ECM, contain a core composed of actin, the actin-binding protein cortactin, the adapter protein Tks5 and actin regulatory proteins such as N-WASP, Arp2/3, cofilin and dynamin [3,4]. Mature invadopodia contain phosphorylated cortactin and adapter proteins as well as Nck and p130Cas, and are surrounded by cell adhesion proteins including β1-integrins and paxillin [2,3,5]. Mature invadopodia utilize the microtubule cytoskeleton to deliver metalloproteinases (MMPs and ADAMs) to invadopodia tips, enabling ECM degradation [3,4,6].

Class IA PI3Ks play a critical role in invadopodia maturation [7–9]. Class IA PI3Ks are heterodimers containing a catalytic subunit (p110α, p110β, p110δ) bound to a regulatory subunit (p85α, p85β, p55α, p50α, p55γ) and are activated downstream of receptor tyrosine kinases (RTKs) and G protein-coupled receptors (GPCRs) [10]. PI3Kβ (a heterodimer containing p85 and p110β) is unique among class IA PI3Ks in that it is regulated by p85 binding to RTKs and by p110β binding to Gβγ, Rab5, Rac1 and Cdc42 [11]. Upon activation, PI3Kβ is recruited to the plasma membrane leading to the production of $PI(3,4,5)P_3$ (PIP_3) and the recruitment

Abbreviations
DiC8, di-octanoyl; ECM, extracellular matrix; EGF, epidermal growth factor; GPCR, G protein coupled receptors; PH domain, pleckstrin homology domain; PI(3)P, phosphatidylinositol 3-phosphate; PI(3,4)P2, phosphatidylinositol (3,4)-diphosphate; PI(3,5)P2, phosphatidylinositol (3,5)-diphosphate; PI(4,5)P2, phosphatidylinositol (4,5)-diphosphate; PI3K, phosphoinositide 3-kinase; PI4KIIβ, phosphatidylinositol 4-kinsae type 2 beta; PIP3, phosphatidylinositol (3,4,5)-triphosphate; PTX, pertussis toxin; RTK, receptor tyrosine kinase; SYNJ2, synaptojanin-2.

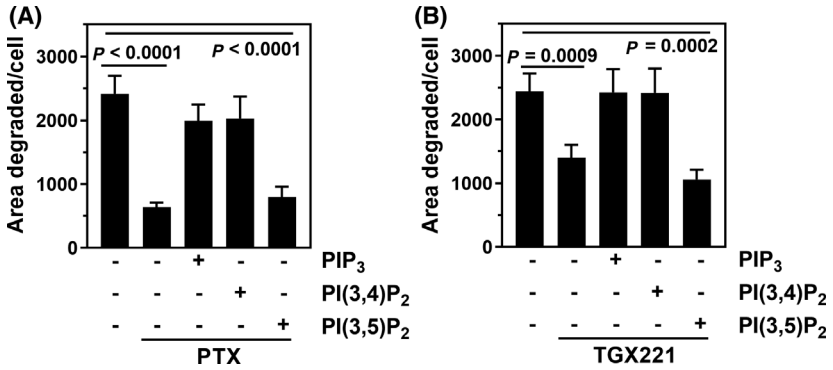

Fig. 1. diC8-PIP_3 and diC8-$PI(3,4)P_2$ rescue gelatin degradation in PTX- and TGX-treated MDA-MB-231 cells. (A) Gelatin degradation was measured in parental MDA-MB-231 cells treated with PTX in the absence or presence of diC8-phosphoinositides. (B) Gelatin degradation was measured in parental MDA-MB-231 cells treated with TGX221 in the absence or presence of diC8-PIP_3,-$PI(3,4)P_2$, or -$PI(3,5)P_2$. Data are the mean ± SEM from 4 or 3 independent experiments, respectively.

of downstream effectors that contain Pleckstrin homology (PH) domains [12]. PIP_3 is converted to $PI(3,4)P_2$ by the phosphoinositide 5′-phosphatases SHIP2 and synaptojanin-2 (SYNJ2) [13,14]. The conversion of PIP_3 to $PI(3,4)P_2$ recruits distinct downstream effectors such as Tks5 and lamellipodin to the invadopod, which are required for invadopodia maturation [7,15].

Our laboratory previously showed that PI3Kβ is selectively required for invadopodia-mediated matrix degradation by MDA-MB-231, BT549 and MDA-MB-468 breast cancer cells [7,16]. PI3Kβ is not required for the formation of invadopodial precursors (measured by cortactin-F-actin punctae that do not colocalize with degraded gelatin) but is required for invadopodial maturation (measured by cortactin-F-actin punctae colocalized with gelatin degradation) [7]. The selective requirement for PI3Kβ during invadopod maturation may be due in part to its involvement in integrin-stimulated responses [7], as integrin activation is required for invadopodia maturation [2,5].

The requirement for PI3Kβ for $PI(3,4)P_2$ production during integrin-stimulated invadopodia maturation is not understood, but could reflect the localization of PI3Kβ to regions of the cell that contain SHIP2. However, in cells expressing activated mutants of PI3K, it is possible that overall increases in PIP_3 production could bypass the requirement for PI3Kβ. Using short-chain soluble phosphoinositides and activated PI3Kβ and PI3Kα mutants, we show that increases in PIP_3 production are sufficient to overcome inhibition of PI3Kβ with regard to invadopodia-mediated gelatin degradation, regardless of the source of the lipids. These data have important implications for the use of PI3Kβ inhibition in tumours that express activated PI3Kα.

Results

Short-chain phosphoinositides rescue gelatin degradation in PTX- or TGX221-treated MDA-MB-231 cells

To manipulate PIP_3 levels in the cell independently of PI3Kβ localization, we used short-chain phosphoinositides (di-octanoyl; C8) that can be added directly to cells to induce signalling functions [17,18]. We used these lipids to bypass inhibition of PI3Kβ by pertussis toxin (PTX), which blocks GPCR activation of PI3Kβ, or by the PI3Kβ-selective kinase inhibitor TGX221. Treatment of MDA-MB-231 cells with PTX blocks gelatin degradation (Fig. 1A). However, degradation

Fig. 2. Treatment of cells with diC8-PIP_3 leads to an increase in plasma membrane $PI(3,4)P_2$. HEK293A cells were transfected with reporters for $PI(3,4)P_2$ (mNeonGreen-cPHx3) or PIP_3 (mCherry-aPHx2). (A) Representative images from time lapse movies of cells expressing the $PI(3,4)P_2$ and PIP_3 reporters and stimulated with EGF. (B) Cells were treated with EGF or diC8-phosphoinositides for 15 min; images were taken every 30 s and stimuli were added after 2 min of imaging. The ratio of plasma membrane to cytosolic fluorescence intensity was calculated as described [19]. The data are the mean ± SEM from 3 independent experiments, n = 29–34 cells. (C) Cells were incubated with EGF or diC8-phosphoinositides for 15-22h. The ratio of plasma membrane to cytosolic fluorescence intensity was compared to data from Fig. 2A taken at 1 min, before the stimuli were added. P-values were obtained by Kruskal–Wallis tests using an alpha of 0.05. The data are pooled from 3 independent experiments, n = 31–35 cells.

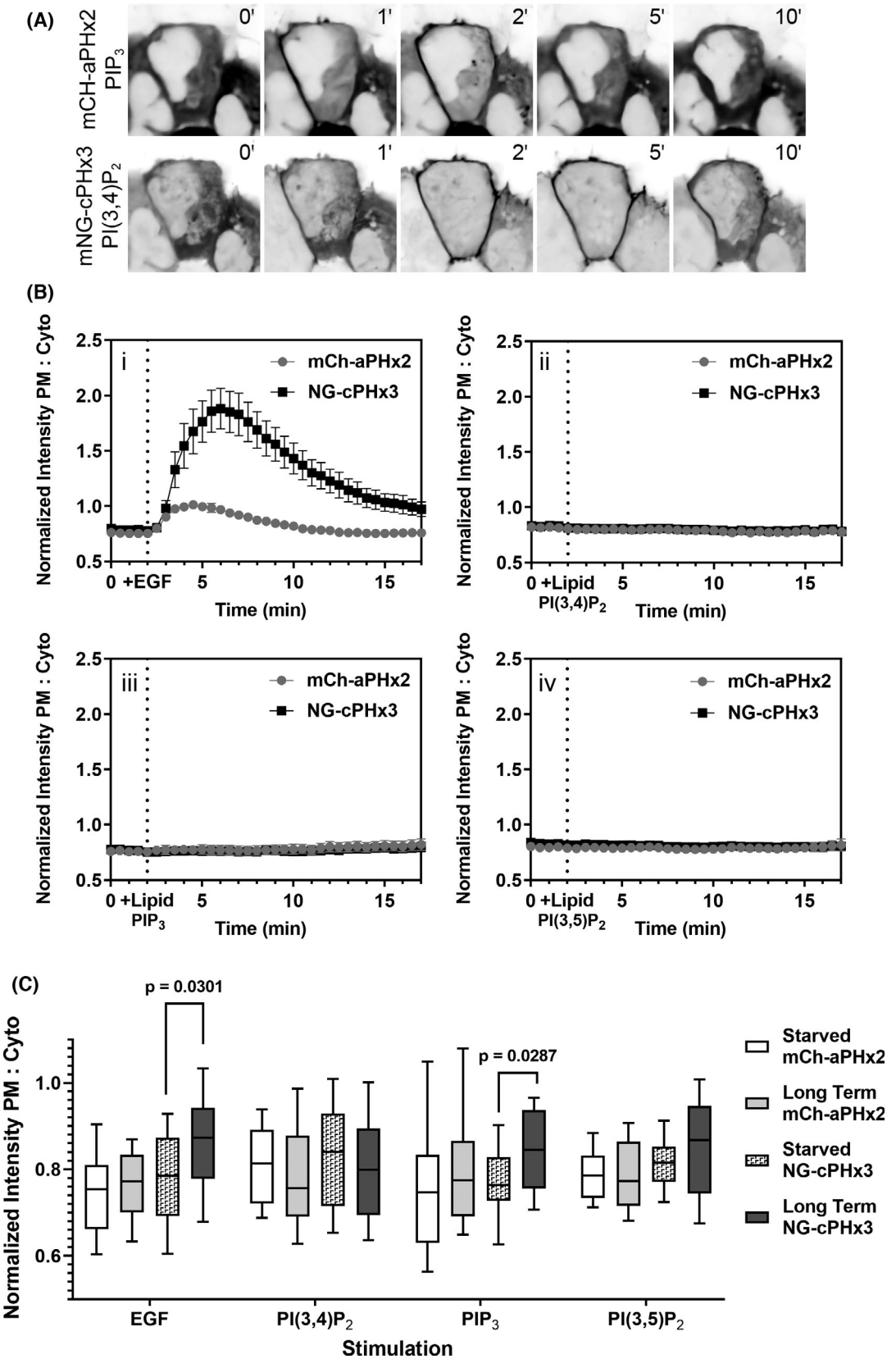
(A)
mCH-aPHx2 PIP3
mNG-cPHx3 PI(3,4)P2
0'
1'
2'
5'
10'
(B)
Normalized Intensity PM : Cyto
i
ii
iii
iv
mCh-aPHx2
NG-cPHx3
0 +EGF
0 +Lipid PI(3,4)P2
0 +Lipid PIP3
0 +Lipid PI(3,5)P2
Time (min)
(C)
p = 0.0301
p = 0.0287
Starved mCh-aPHx2
Long Term mCh-aPHx2
Starved NG-cPHx3
Long Term NG-cPHx3
EGF
PI(3,4)P2
PIP3
PI(3,5)P2
Stimulation

was rescued by the addition of diC8-PIP_3 or diC8-PI(3,4)P_2, but not diC8-PI(3,5)P_2. Similar results were obtained in cells treated with TGX221 (Fig. 1B).

Interestingly, PIP_3 and PI(3,4)P_2 showed similar potency in the rescue of gelatin degradation; dose responses showed maximal rescue at a concentration of 1 μM for both lipids (data not shown). Given that invadopodia maturation requires PI(3,4)P_2, this suggested that diC8-PIP_3 was efficiently converted to PI(3,4)P_2 during the 18-h gelatin degradation assay. We examined this in two ways. First, we used a previously described fluorescent biosensor for PI(3,4)P_2 to measure intracellular levels of this lipid after incubation of cells with diC8-phosphoinositides [19]. Unlike acute stimulation with EGF, which produced increases in both PI(3,4)P_2 and PIP_3, acute stimulation with diC8-PIP_3 produced no detectable signal (Fig. 2A-B). However, chronic stimulation with diC8-PIP_3 led to a significant increase in PI(3,4)P_2 in the plasma membrane (Fig. 2C). These data suggest that diC8-PIP_3 partitions slowly across the cell membrane, where it is efficiently converted to diC8-PI(3,4)P_2. We could not detect increases in plasma membrane PI(3,4)P_2 after chronic incubation of cells with diC8-PI(3,4)P_2.

In a parallel approach, we tested whether the rescue of gelatin degradation by diC8 lipids required SHIP2. We first treated cells with the SHIP2 inhibitor AS1949490, which blocked gelatin degradation in MDA-MB-231 cells (Fig. 3A). Gelatin degradation in AS1949490-treated cells was rescued by diC8-PI(3,4)P_2, but not diC8-PIP_3, showing that PIP_3 cannot drive matrix degradation in the absence of SHIP2 activity. Similarly, we treated cells with PTX to block PI3Kβ activation and inhibit gelatin degradation (Fig. 3B). While gelatin degradation was rescued by diC8-PIP_3, this rescue was abrogated when cells were co-treated with the SHIP2 inhibitor AS1949490 (Fig. 3B). Together, these results suggest that diC8-PIP_3 must be converted to diC8-PI(3,4)P_2 to rescue invadopodia activity and gelatin degradation.

Activating PIK3CB and PIK3CA mutants rescue gelatin degradation in cells treated with PTX

To increase cellular PIP_3 levels using an orthogonal approach, we next tested whether expression of the constitutively active p110β mutants D1067Y [20] or E1051K [21] would rescue gelatin degradation in PTX-treated cells. Stable expression of the mutants in MDA-MB-231 cells led to robust Akt activation (Fig. 4A,B), demonstrating that the p110β mutants increased PI3K signalling. Similarly, increases in both PI(3,4)P_2 and PIP_3 could be detected using fluorescent biosensors in cells expressing mutant p110β (Fig. 4C). Whereas the treatment of control MDA-MB-231 cells with PTX reduced gelatin degradation, cells expressing the E1051K and D1067Y activating mutations were unaffected by PTX (Fig. 4D).

The ability of diC8-PIP_3 to rescue gelatin degradation in TGX221-treated cells (Fig. 1B) suggested that rescue by constitutively active PI3Kβ mutants might not be isotype selective. We therefore stably expressed wild-type or constitutively active (H1047R and E545K) p110α in MDA-MB-231 cells [22]. Overexpression of both mutants led to increased Akt activation (Fig. 5A-B). An increase in plasma membrane PIP_3 and PI(3,4)P_2 was also detected with the H1047R mutant, although not with the E545K mutant (Fig. 4C); the reason for this difference is not clear but could reflect differential signalling by the two mutants [22]. Expression of H1047R but not wild-type p110α overcame the inhibition of gelatin degradation by PTX (Fig. 5C). Similarly, TGX221 failed to inhibit gelatin degradation in cells overexpressing either wild-type or H1047R p110α (Fig. 5E). Consistent with our data with C8 lipids (Fig. 3), gelatin degradation in cells

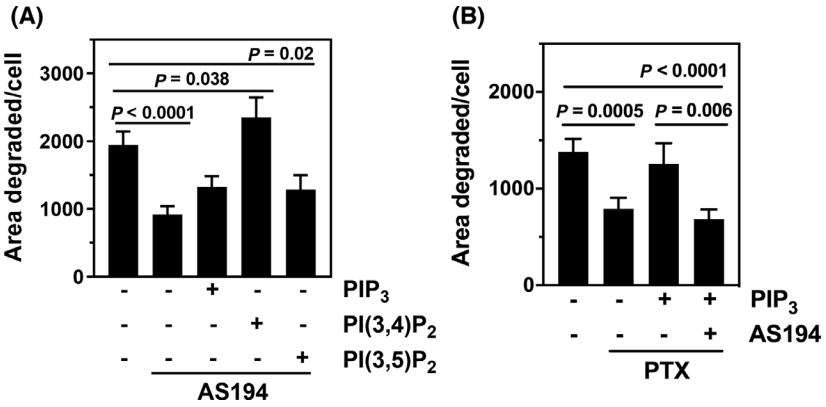

Fig. 3. diC8-PI(3,4)P_2 but not diC8-PIP_3 rescues gelatin degradation in MDA-MB-231 cells treated with SHIP2 inhibitor. (A) Gelatin degradation was measured in parental MDA-MB-231 cells treated with AS1949490 in the absence or presence of diC8-phosphoinositides. (B) Gelatin degradation was measured in parental MDA-MB-231 cells treated with PTX alone or co-treated with PTX and AS1949490, in the absence or presence of diC8-PIP_3. The data are the mean ± SEM from 3 independent experiments.

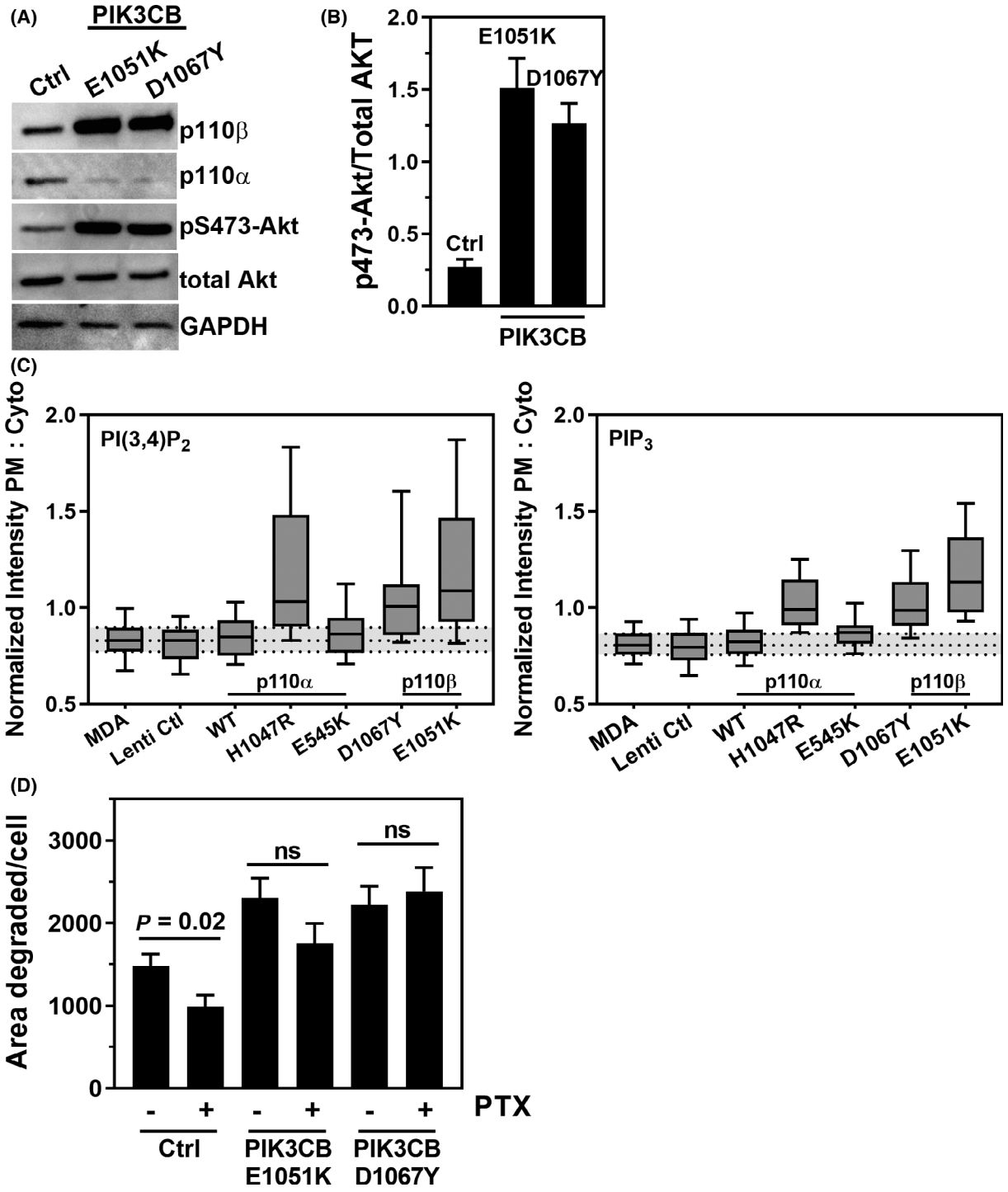

Fig. 4. Activating PIK3CB mutants rescue gelatin degradation in PTX-treated cells. (A) Lysates from lentivirus control MDA-MB-231 cells, or cells stably overexpressing E1051K or D1067Y p110β were blotted for p110β, p110α, pS473-AKT, total AKT and GAPDH. (B) Western blots were quantitated using a Kodak Image Station 4000R. The data are the mean ± SEM from 3 independent experiments. (C) MDA-MB-231 cells stably expressing E1051K p110β, D1067Y p110β, E545K p110α or H1047R p110α were transfected with reporters for PI(3,4)P_2 (mNeonGreen-cPHx3) or PIP_3 (mCherry-aPHx2). The ratio of plasma membrane to cytosolic fluorescence intensity was calculated as described [19]. The data are the mean ± SEM from 3 independent experiments, n = 49–58 cells. (D) Gelatin degradation was measured in control, PIK3CB E1051K and PIK3CB D1067Y MDA-MB-231 cells treated without or with PTX. The data are the mean ± SEM from 3 independent experiments.

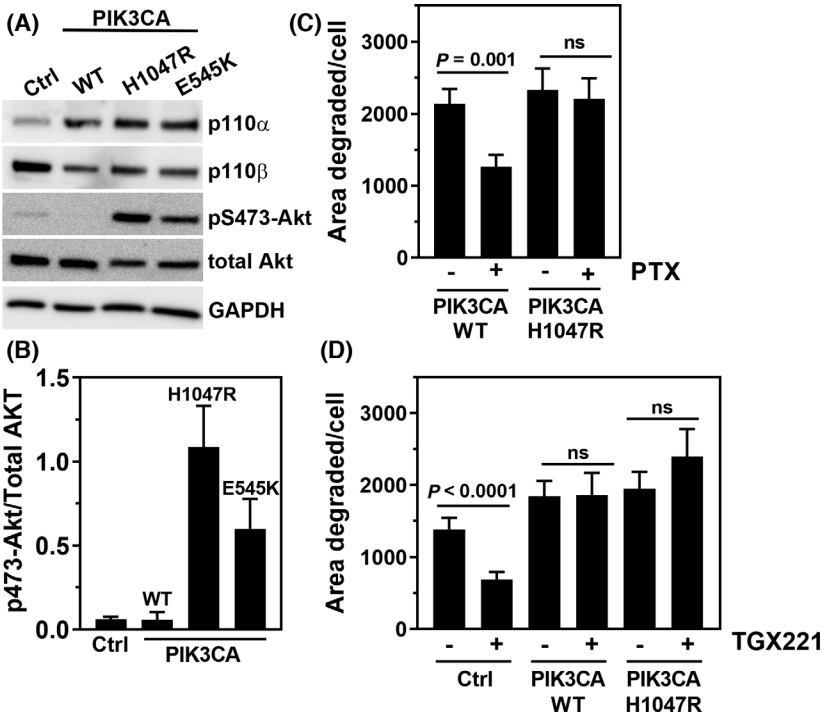

Fig. 5. Activating PIK3CA mutation rescues gelatin degradation in PTX- and TGX221-treated cells. (A) Lysates from parental MDA-MB-231 cells or cells stably overexpressing WT, H1047R, or E545K p110α were blotted for p110β, p110α, pS473-AKT, total AKT and GAPDH. (B) Western blots were quantitated as above. The data are the mean ± SEM from 3 independent experiments. (C) Gelatin degradation was measured in MDA-MB-231 cells overexpressing WT or H1047R p110α and treated without or with PTX. The data are the mean ± SEM from 3 independent experiments. (D) Gelatin degradation was measured in parental MDA-MB-231 cells or cells overexpressing WT or H1047R p110α, and treated without or with TGX221. The data are the mean ± SEM from 3 independent experiments.

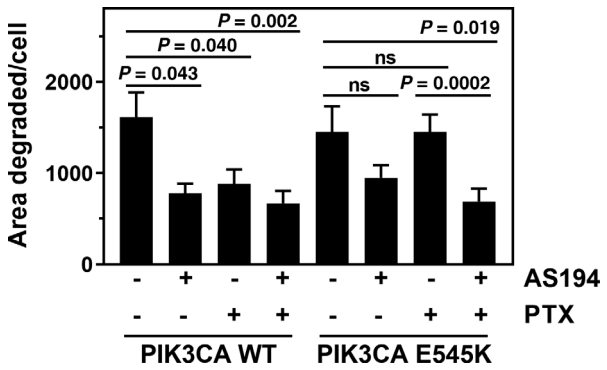

Fig. 6. Rescue of gelatin degradation in PTX-treated cells by an activating PIK3CA mutant requires SHIP2 activity. Gelatin degradation was measured in MDA-MB-231 cells overexpressing WT or E545K p110α and treated with PTX, AS1949490 or both. The data are the mean ± SEM from 2 independent experiments.

expressing E545K p110α was unaffected by PTX but was blocked by treatment of cells with the SHIP2 inhibitor (Fig. 6).

Discussion

Our data, along with published work from other laboratories, support a model in which invadopodial maturation requires the SHIP2-dependent conversion of PIP$_3$ to PI(3,4)P$_2$ [15–17]. We have also previously shown that the PI3Kβ isotype is selectively required for the production of PI(3,4)P$_2$ in invadopodia [7]. The mechanism for coupling between PI3Ks and SHIP2 is not known. PI3Kβ binds to CRKL in PTEN-deficient tumour cells [23]. This could recruit PI3Kβ to integrin-associated scaffolds such as p130Cas [24] and Nedd9 [25], which also bind to SHIP2 [24,26]. Alternatively, independent of its localization, PI3Kβ could be preferentially activated during matrix degradation, to produce more PIP$_3$ than other isotypes. In neutrophils, PIP$_3$ production by PI3Kβ exceeds that of other Class I PI3Ks under conditions of maximal activity (resulting from simultaneous RTK and GPCR activation) [9]. Integrins are known to couple to tyrosine kinases that lead to activation of PI3K [27–29], and we have shown a requirement for Gβγ binding to PI3Kβ during invadopodia maturation [7,16]. These data suggest that PI3Kβ in invadopodia could be subject to a maximally activating combined RTK/GPCR stimulus.

Despite the mechanism for selective PI3Kβ-SHIP2 coupling in tumour cells, this selectivity can be overcome when PIP$_3$ levels are increased by pharmacological treatments or mutational pathway activation. Our data show that the reduction in gelatin degradation caused by PTX or TGX221 treatment is rescued by the addition of diC8-PI(3,4)P$_2$ or diC8-PIP$_3$, or by the expression of constitutively active PI3Kβ or PI3Kα. Consistent with our earlier results [7], rescue by either method is dependent on SHIP2 activity.

The behaviour of diC8 lipids in cells is not fully understood. Acute addition of either diC8-PIP_3 or diC8-PI(3,4)P_2 has no detectable effect on the recruitment of PH domain probes to the membrane, suggesting that they do not rapidly reach the cell interior. In contrast, 18-h treatment of PIP_3 led to a significant increase in plasma membrane PI(3,4)P_2. This observation suggests that diC8-PIP_3 partitions slowly into the inner leaflet of the plasma membrane, where it is converted to diC8-PI(3,4)P_2. While we were unable to detect the appearance of diC8-PI(3,4)P_2 after an 18-h incubation, the lipids clearly accumulate to levels sufficient to promote invadopodia function, as it rescues gelatin degradation in cells treated with PTX or the PI3Kβ inhibitor TGX221. It is unlikely that the effects of diC8-PI(3,4)P_2 on matrix degradation are due to its conversion to diC8-PI(3)P and diC8-PI(4)P. While MDA-MB-231 cells do not express INPP4B, which hydrolyses PI(3,4)P_2 to PI(3)P [30], they do express PTEN, which hydrolyses PI(3,4)P_2 to PI(4)P [31,32]. However, knockdown of PI4KIIα has no effect on invadopodia and knockdown PI4KIIβ induces invadopodia [33]. Finally, it is also possible that the effective lifetime of diC8-PI(3,4)P_2 is longer in MDA-MB-231 than in HEK293A cells due to lack of INPP4B in MDA-mB-231 cells [30].

Our previously published data suggest that PI3Kβ inhibitors might be useful to inhibit tumour cell invasion during metastasis [7,16]. Our study suggests that activating mutations of PIK3CA might bypass the requirement for PI3Kβ in invadopodia, by elevating PIP_3 levels and PIP_3 conversion to PI(3,4)P_2. This is analogous to the loss of PI3Kβ-dependent growth in PTEN-null tumours that also express mutations that activate PI3Kα [34]. These experiments highlight the importance of determining the genetic features of a tumour to develop effective therapeutics against tumour metastasis.

Material and methods

Antibodies and reagents

Antibodies to GAPDH (2118), p110β (3011), p110α (4249), pS473-Akt (4060) and total Akt (9272) were purchased from Cell Signaling Technology. Rhodamine-phalloidin (R415) was purchased from Invitrogen. Poly-L-lysine (0.01%; P4707) and gelatin from porcine skin type A (G2625) were purchased from Sigma. Glutaraldehyde was purchased from Electron Microscopy Sciences. Formaldehyde was purchased from Invitrogen. DAPI Fluoromount-G was purchased from Southern Biotech and was used for mounting coverslips. TGX221 was purchased from Selleckchem. AS1949490 was purchased from Sigma. Pertussis toxin was purchased from Millipore. Oregon Green 488-conjugated gelatin (G13186) was purchased from Invitrogen. diC8-PI(3,4)P_2, (P3408), diC8-PIP_3 (P3908) and diC8-PI(3,5)P_2 (P3508) were purchased from Echelon Biosciences and were reconstituted in sterile water to a final concentration of 1 mM.

Cell culture

The human breast cancer cell line MDA-MB-231 was obtained from the American Type Culture Collection. MDA-MB-231 cells were cultured in DMEM containing 10% FBS at 37 °C and 5% CO_2. Lentivirus-infected cell lines were maintained in 2 $\mu g \cdot mL^{-1}$ puromycin.

DNA constructs, Virus production and transductions

MDA-MB-231 cells overexpressing wild-type or constitutively active PIK3CA were described previously [22]. pHAGE-PIK3CB-E1051K (116553), pHAGE-PIK3CB-D1067Y (116551) and helper and packaging constructs pMD2.6 (23359) and psPAX2 (12260) were purchased from Addgene. Lentiviruses were produced by transfecting HEK293T cells with the PIK3CB constructs along with pMD2.6 and psPAX2 using Lipofectamine 3000 (Invitrogen, Waltham, MA, USA). After 24 h, viral supernatants were filtered with a 0.45-μm filter. MDA-MB-231 cells were infected with virus and selected with puromycin (4 $\mu g \cdot mL^{-1}$). The expression of p110β was verified by western blot. For cell lines expressing constitutively active PI3K, activation was evaluated by measuring pS473-Akt.

Western blotting

Cells were plated on 60-mm gelatin-coated tissue culture dishes. The tissue culture dishes were coated with 0.01% poly-L-lysine for 10 min at room temperature and then washed three times with PBS. The dishes were treated with 0.5% glutaraldehyde for 10 min, washed 5 times with PBS and then incubated with 0.2% gelatin diluted in PBS for 30 min at 37 °C. The dishes were then treated with 0.1 M glycine for 10 min at room temperature, washed twice with PBS and then seeded with cells. Cells were lysed in Laemmli buffer lacking bromophenol blue and supplemented with 100 μM PMSF, 1 $\mu g \cdot mL^{-1}$ leupeptin, 1 $\mu g \cdot mL^{-1}$ aprotinin, 1 mM DTT and 1:100 phosphatase inhibitor cocktails 2 (P5726) and 3 (P0044) from Sigma. Cell lysates were boiled for 5 min at 100 °C and sonicated. Protein concentrations were determined using the Bio-Rad DC protein assay kit. 30 μg of lysate was mixed with Laemmli sample buffer containing 200 mM DTT, boiled at 100 °C for 5 min and analysed by SDS/PAGE and western blotting with the Super Signal West Pico PLUS Chemiluminescent Substrate (Thermo Scientific, Waltham, MA, USA). Gels were imaged using a Kodak Image Station 4000R.

Gelatin degradation assay

The gelatin degradation assay was performed as described previously [16]. In brief, acid-washed coverslips were coated with 0.01% poly-L-lysine, cross-linked with 0.5% glutaraldehyde, coated with 200 $\mu g \cdot mL^{-1}$ Oregon Green 488-conjugated gelatin for 15 min and quenched with 0.1 M glycine. For experiments with diC8 lipids (1 μM) or inhibitors (500 nM TGX221 or 10 μM AS1949490), cells were pretreated for 30 min before seeding. For experiments using PTX (200 $ng \cdot mL^{-1}$), cells were pre-treated for 15 h before seeding. 8.5×10^4 cells were seeded on Oregon Green 488-conjugated gelatin coated coverslips, incubated for 18 h in the presence of lipids or inhibitors, fixed with 4% formaldehyde and permeabilized with 0.05% Triton X-100. Cells were stained with Rhodamine-phalloidin and mounted using DAPI Fluoromount-G. For the gelatin degradation assay, images were acquired with a 60× 1.4 NA objective on a Nikon Eclipse E400 microscope. For quantification of the fluorescent gelatin images, the background was subtracted with a rolling ball radius of 20. The images were thresholded to define areas of degradation per cell, which was measured in IMAGEJ.

Live-cell imaging of diC_8-lipid loaded cells

HEK293A cells (RRID:CVCL_6910) grown in DMEM supplemented with 10% FBS, 100 $\mu \cdot mL^{-1}$ penicillin, 10 $\mu g \cdot mL^{-1}$ streptomycin and 0.1% chemically defined lipid supplement (Thermo Fisher) were seeded into #1.5 22-mm-diameter glass-bottom 35-mm dishes (CellVis) coated with 20 $\mu g \cdot mL^{-1}$ entactin-collagen-laminin mix. At least 1 h postseeding, cells were transfected with 0.8 μg mNeonGreen-cPHx3 and 0.2 μg mCherry-aPHx2 plasmids pre-incubated for > 5 min with 3 μg lipofectamine 2000 in 200 μL Opti-MEM. Transfection media was replaced after 3–4 h with Fluorobrite medium (Thermo Fisher) supplemented with 0.1% BSA and 0.1% chemically defined lipid supplement. As indicated in the figure, EGF or diC_8 lipids were added to 20 $ng \cdot mL^{-1}$ or 1 μM, respectively. Immediately prior to imaging, cells were stained with the selective plasma membrane dye Cell Mask Deep Red at 1 $\mu g \cdot mL^{-1}$ for 5 min before rinsing. Imaging was performed 24 h post-transfection on a Nikon A1R resonant scanning confocal microscope using a 1.45 NA, 100× plan-apochromatic objective lens mounted on a Nikon Ti-inverted microscope stand. The confocal pinhole was set to acquire at a resolution of 1.2 airy units on the far-red channel. Green (mNeonGreen), red (mCherry) and far-red (Cell Mask) fluorescence were excited with 488 nm, 561 nm and 640 nm diode lasers on sequential scans and detected on separate photomultiplier tubes equipped with appropriate dichroic and emission optics (500–550 nm for green, 570–620 nm for red, 663–737 nm for far red).

Image analysis

Images saved in Nikon.nd2 format were opened using the LOCI bioformats importer for FIJI. Cell-specific regions of interest (ROI) were drawn around whole cells and on small regions of cytoplasm. The Cell Mask channel was used to define a mask of the plasma membrane using an auto thresholding approach, based on wavelet decompositions across three wavelength-defined length scales as detailed in [35]. Next, the masked region of plasma membrane in the green and red channels was normalized to the intensity of the cytoplasmic ROI in the same cells, defining the PM:Cyto ratio. This ratio was measured for each cell across all recorded time points.

Statistical analysis

All statistical analyses were performed using GRAPHPAD Prism version 8. Statistical analyses were designed in consultation with the Einstein Biostatistics core. If the primary data, or the log2 transformation was normally distributed, a *t*-test or ANOVA was used. If the data were not normally distributed and a Kruskal–Wallis test produced a significant result, p-values were generated using the Mann–Whitney *U* test.

Conflict of interest

The authors declare no conflict of interest.

Data accessibility

Raw data, cell lines and plasmids are available by contacting the corresponding author.

Acknowledgement

This work was supported by DOD grant BC181067 (JMB), T32 GM7288 (CTJ) and NIGMS 1R35GM119412 (GRVH).

Author contributions

CTJ and CCW performed experimental data; CTJ, CCW, GRVH, ARB and JMB wrote and edited the manuscript; GRVH, ARB and JMB supervised the article; ARB, JMB and GRVH performed funding acquisition.

References

1 Leong HS, Robertson AE, Stoletov K, Leith SJ, Chin CA, Chien AE et al. Invadopodia are required for cancer cell extravasation and are a therapeutic target for metastasis. *Cell Rep*. 2014;**8**:1558–70.
2 Beaty BT, Sharma VP, Bravo-Cordero JJ, Simpson MA, Eddy RJ, Koleske AJ et al. β1 integrin regulates Arg to promote invadopodial maturation and matrix degradation. *Mol Biol Cell*. 2013;**24**:1661–75.

3 Eddy RJ, Weidmann MD, Sharma VP, Condeelis JS. Tumor cell invadopodia: invasive protrusions that orchestrate metastasis. *Trends Cell Biol*. 2017;**27**:595–607.
4 Murphy DA, Courtneidge SA. The 'ins' and 'outs' of podosomes and invadopodia: characteristics, formation and function. *Nat Rev Mol Cell Biol*. 2011;**12**:413.
5 Branch KM, Hoshino D, Weaver AM. Adhesion rings surround invadopodia and promote maturation. *Biol Open*. 2012;**1**:711–22.
6 Beaty BT, Condeelis J. Digging a little deeper: the stages of invadopodium formation and maturation. *Eur J Cell Biol*. 2014;**93**:438–44.
7 Erami Z, Heitz S, Bresnick AR, Backer JM. PI3Kbeta links integrin activation and PI(3,4)P2 production during invadopodial maturation. *Mol Biol Cell*. 2019;**30**:276.
8 Yamaguchi H, Yoshida S, Muroi E, Yoshida N, Kawamura M, Kouchi Z et al. Phosphoinositide 3-kinase signaling pathway mediated by p110alpha regulates invadopodia formation. *J Cell Biol*. 2011;**193**:1275–88.
9 Houslay DM, Anderson KE, Chessa T, Kulkarni S, Fritsch R, Downward J et al. Coincident signals from GPCRs and receptor tyrosine kinases are uniquely transduced by PI3Kβ in myeloid cells. *Sci Signal*. 2016;**9**:ra82.
10 Burke JE, Williams RL. Synergy in activating class I PI3Ks. *Trends Biochem Sci*. 2015;**40**:88–100.
11 Bresnick AR, Backer JM. PI3Kβ–a versatile transducer for GPCR, RTK and small GTPase signaling. *Endocrinology*. 2019;**160**:536–55.
12 Thorpe LM, Yuzugullu H, Zhao JJ. PI3K in cancer: divergent roles of isoforms, modes of activation and therapeutic targeting. *Nat Rev Cancer*. 2015;**15**:7–24.
13 Suwa A, Kurama T, Shimokawa T. SHIP2 and its involvement in various diseases. *Expert Opinion Therap Targ*. 2010;**14**:727–37.
14 Ben-Chetrit N, Chetrit D, Russell R, Korner C, Mancini M, Abdul-Hai A et al. Synaptojanin 2 is a druggable mediator of metastasis and the gene is overexpressed and amplified in breast cancer. *Sci Signal*. 2015;**8**:ra7.
15 Sharma VP, Eddy R, Entenberg D, Kai M, Gertler FB, Condeelis J. Tks5 and SHIP2 regulate invadopodium maturation, but not initiation, in breast carcinoma cells. *Curr Biol*. 2013;**23**:2079–89.
16 Khalil BD, Hsueh C, Cao Y, Saab WFA, Wang Y, Condeelis JS et al. GPCR signaling mediates tumor metastasis via PI3Kβ. *Cancer Res*. 2016;**1675**:2015.
17 Ghosh S, Scozzaro S, Ramos AR, Delcambre S, Chevalier C, Krejci P et al. Inhibition of SHIP2 activity inhibits cell migration and could prevent metastasis in breast cancer cells. *J Cell Sci*. 2018;**131**.
18 Viaud J, Lagarrigue F, Ramel D, Allart S, Chicanne G, Ceccato L et al. Phosphatidylinositol 5-phosphate regulates invasion through binding and activation of Tiam1. *Nat Commun*. 2014;**5**:4080.
19 Goulden BD, Pacheco J, Dull A, Zewe JP, Deiters A, Hammond GRV. A high-avidity biosensor reveals plasma membrane PI(3,4)P2 is predominantly a class I PI3K signaling product. *J Cell Biol*. 2019;**218**:1066–79.
20 Nakanishi Y, Walter K, Spoerke JM, O'Brien C, Huw LY, Hampton GM et al. Activating Mutations in PIK3CB Confer Resistance to PI3K Inhibition and Define a Novel Oncogenic Role for p110beta. *Cancer Res*. 2016;**76**:1193–203.
21 Whale AD, Colman L, Lensun L, Rogers HL, Shuttleworth SJ. Functional characterization of a novel somatic oncogenic mutation of PIK3CB. *Signal Transduct Target Ther*. 2017;**2**:17063.
22 Pang H, Flinn R, Patsialou A, Wyckoff J, Roussos ET, Wu H et al. Differential enhancement of breast cancer cell motility and metastasis by helical and kinase domain mutations of class IA phosphoinositide 3-kinase. *Cancer Res*. 2009;**69**:8868–76.
23 Zhang J, Gao X, Schmit F, Adelmant G, Eck MJ, Marto JA et al. CRKL mediates p110β-dependent PI3K signaling in PTEN-deficient cancer cells. *Cell Rep*. 2017;**20**:549–57.
24 Prasad N, Topping RS, Decker SJ. SH2-containing inositol 5′-phosphatase SHIP2 associates with the p130Cas adapter protein and regulates cellular adhesion and spreading. *Mol Cell Biol*. 2001;**21**:1416–28.
25 Hamze-Komaiha O, Sarr S, Arlot-Bonnemains Y, Samuel D, Gassama-Diagne A. SHIP2 regulates lumen generation, cell division, and ciliogenesis through the control of basolateral to apical lumen localization of aurora A and HEF 1. *Cell Rep*. 2016;**17**:2738–52.
26 Chodniewicz D, Klemke RL. Regulation of integrin-mediated cellular responses through assembly of a CAS/Crk scaffold. *Bba-Mol Cell Res*. 2004;**1692**:63–76.
27 King WG, Mattaliano MD, Chan TO, Tsichlis PN, Brugge JS. Phosphatidylinositol 3-kinase is required for integrin-stimulated AKT and Raf-1/mitogen-activated protein kinase pathway activation. *Mol Cell Biol*. 1997;**17**:4406–18.
28 Manganaro D, Consonni A, Guidetti GF, Canobbio I, Visconte C, Kim S et al. Activation of phosphatidylinositol 3-kinase beta by the platelet collagen receptors integrin alpha2beta1 and GPVI: The role of Pyk2 and c-Cbl. *Bba-Mol Cell Res*. 2015;**1853**:1879–88.
29 Genna A, Lapetina S, Lukic N, Twafra S, Meirson T, Sharma VP et al. Pyk2 and FAK differentially regulate invadopodia formation and function in breast cancer cells. *J Cell Biol*. 2018;**217**:375–95.
30 Fedele CG, Ooms LM, Ho M, Vieusseux J, O'Toole SA, Millar EK et al. Inositol polyphosphate 4-phosphatase II regulates PI3K/Akt signaling and is lost

in human basal-like breast cancers. *Proc Natl Acad Sci USA*. 2010;**107**:22231–6.
31 Malek M, Kielkowska A, Chessa T, Anderson KE, Barneda D, Pir P et al. PTEN regulates PI(3,4)P2 signaling downstream of class I PI3K. *Mol Cell*. 2017;**68**:566–80.
32 Reed DE, Shokat KM. INPP4B and PTEN Loss Leads to PI-3,4–P2 Accumulation and Inhibition of PI3K in TNBC. *Mol Cancer Res*. 2017;**15**:765–75.
33 Alli-Balogun GO, Gewinner CA, Jacobs R, Kriston-Vizi J, Waugh MG, Minogue S. Phosphatidylinositol 4-kinase IIbeta negatively regulates invadopodia formation and suppresses an invasive cellular phenotype. *Mol Biol Cell*. 2016;**27**:4033–42.
34 Schmit F, Utermark T, Zhang S, Wang Q, Von T, Roberts TM et al. PI3K isoform dependence of PTEN-deficient tumors can be altered by the genetic context. *Proc Natl Acad Sci USA*. 2014;**111**:6395–400.
35 Wills RC, Pacheco J, Hammond GRV. Quantification of Genetically Encoded Lipid Biosensors. *Methods Mol Biol*. 2021;**2251**:55–72.